

Tunable-Focus Cylindrical Liquid Crystal Lenses

Yi-Hsin LIN, Hongwen REN, Kuan-Hsu FAN-CHIANG¹, Wing-Kit CHOI, Sebastian GAUZA, Xinyu ZHU and Shin-Tson WU*

College of Optics and Photonics, University of Central Florida, Orlando, Florida 32816, USA

¹Institute of Electro-Optical Engineering, National Chiao Tung University, Hsinchu, Taiwan 30050, Republic of China

(Received April 6, 2004; revised July 27, 2004; accepted September 29, 2004; published January 11, 2005)

Tunable-focus cylindrical liquid crystal lenses of four different electrode configurations are analyzed. Simulation results show that the proposed devices can have different focal lengths even if they have the same aperture size. A good agreement between experiment and simulation results is obtained. The imaging property of one of the cylindrical liquid crystal lenses is also demonstrated. [DOI: 10.1143/JJAP.44.243]

KEYWORDS: liquid crystal, cylindrical lens, LC lens, tunable focal length

A cylindrical lens focuses light in one dimension. It can be used for stretching an image, focusing light into a slit, converging light for a line scan detector or correcting low-order aberration. A solid cylindrical lens has a fixed focal length. To obtain variable focal length, the use of a set of lenses, *e.g.*, mechanical zoom lens, is often necessary. This however makes the optical system bulky and costly. An alternative approach to obtain variable focal length is the use of liquid-crystal (LC)-based cylindrical lenses for which several methods have been considered and proposed.^{1–8)} Among such lenses, those with slit electrodes are particularly interesting due to their simple fabrication, simple operation, and the possibility of widening their aperture size.

Figure 1 shows eight possible electrode configurations for generating electric fields. However, the two configurations shown in Figs. 1(e) and 1(f) cannot work as a lens due to the absence of an inhomogeneous electric field. The structures in Figs. 1(g) and 1(h) are more suitable for fabricating cylindrical microlens arrays than for fabricating single large-aperture lenses due to their narrow electrode gaps. The aperture size of a micro-cylindrical LC lens is generally in the 100 μm range.^{5,6)} Its application is therefore severely limited. To scale-up the aperture size of such a lens, we previously proposed putting a slit electrode on the outer surface of a substrate.⁸⁾ In this paper, we present four

different electrode structures for a LC cylindrical lens and analyze the performances of the lens by computer simulations. The simulation results agree with the experiment results reasonably well.

To have a wider aperture size of a LC lens, four possible configurations shown in Figs. 1(a) to 1(d) have been considered. In configuration (a), a slit electrode is coated on the outer surface of the top substrate, whereas a continuous electrode is coated on the outer surface of the bottom substrate. In configuration (b), a slit electrode is coated on the outer surface of both top and bottom substrates. The two slits are parallel and symmetrical. In configuration (c), a slit electrode is coated on the outer surface of the top substrate, whereas a continuous electrode is coated on the inner surface of the bottom substrate. In configuration (d), a slit electrode is coated on the outer surface of the top substrate, whereas another slit electrode is coated on the inner surface of the bottom substrate. The two slits are also parallel and symmetrical. Each of the LC cells has the same cell gap $d = 40 \mu\text{m}$. The slit spacing, called the aperture width, of the slit electrode is $a = 2 \text{ mm}$. The inner surfaces of both top and bottom substrates were coated with polyimide and buffed in antiparallel directions along the slit direction. LC molecules are aligned along the slit direction to avoid disclination lines during device operation. The devices were filled with the nematic liquid crystal UCF-B (birefringence $\Delta n = 0.44$).⁹⁾

To investigate LC molecular orientation states in an inhomogeneous electric field, we used the commercial software 2DimMOS (autronic-MELCHERS GMBH) to calculate the LC director profile distribution of the four different LC lens cells mentioned above. The parameters used in the simulations are as follows: dielectric constants $\epsilon_{\parallel} = 14.9$ and $\epsilon_{\perp} = 3.3$, splay elastic constant $K_{11} = 20.3 \text{ pN}$, bend elastic constant $K_{33} = 33.8 \text{ pN}$, extraordinary refractive index $n_e = 1.9653$, and ordinary refractive index $n_o = 1.5253$. We first calculated the effective extraordinary refractive index n_{eff} . The data of the LC director profile for each LC layer was extracted using: $1/n_{\text{eff}}(\theta(V))^2 = \sin^2 \theta(V)/n_o^2 + \cos^2 \theta(V)/n_e^2$, where $\theta(V)$ is the tilt angle of a LC layer at a given applied root-mean-square voltage V_{rms} . We calculated the refractive index difference $dn = n_{\text{eff}}(\theta(V)) - n_o$ for each LC layer and then averaged the results obtained. The effective focal length f of a cylindrical LC lens was then calculated using $f = \pi w^2 / (4\lambda \Delta n)$, where w is the aperture width, λ is the wavelength, and Δn is the

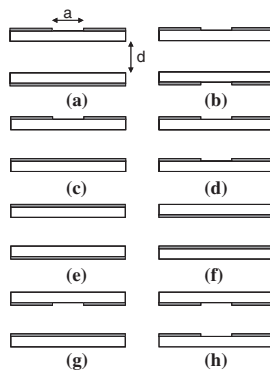


Fig. 1. Eight possible electrode configurations considered for fabricating a cylindrical LC lens. a = slit width and d = cell gap. The rubbing direction is facing outward to the paper, and the polarization of the incident light is along the rubbing direction.

*E-mail address: swu@mail.ucf.edu

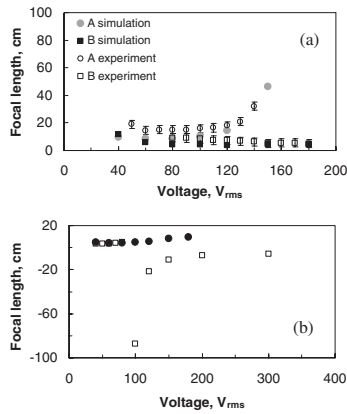


Fig. 2. Voltage-dependent focal length of cylindrical LC lenses: (a) Simulation and experimental results for configurations A and B, (b) Simulation results for configurations C and D. The filled circles in (b) are results for configuration C and the open squares are those for configuration D with a reduced aperture size $a = 1.2$ mm.

phase difference between the center and edge of the aperture.¹⁰⁾

Figure 2(a) shows the calculated and measured voltage-dependent focal lengths of two cylindrical LC lens: configurations A and B. The agreement between the simulation and measurement results is reasonably good. From the simulation results, we found that the LC lens of configuration B has the best positive refractive index profile and the shortest focal length. The LC lens of configuration A has a severe image aberration problem and a larger focal length (> 15 cm) than B due to its broader and shallower refractive index profile. For configuration C [Fig. 2(b)], the simulation minimum focal length occurs at $V \sim 60$ V_{rms} ($f = 1$ KHz), which is consistent with the reported experimental results.⁸⁾ For configuration D, if the aperture size is maintained at 2 mm, the fringing field-induced refractive index profile is far from the ideal parabolic shape. The image quality is poor. Thus, we reduce the aperture to 1.2 mm to obtain a parabolic refractive index profile. The simulation results indicate that both positive and negative lenses can be obtained depending on applied voltage. When $V < 100$ V_{rms}, the lens has a positive focal length, which becomes negative when $V > 100$ V_{rms}. The minimum focal length for the positive lens is ~ 3 cm and the maximum focal length for the negative lens is ~ -5 cm.

To measure the focusing properties, a collimated linearly polarized He-Ne laser beam ($\lambda = 633$ nm) was used to illuminate the LC cells. A charge coupled device (CCD) camera was used to characterize the focusing properties of the lens. A computer controlled LabVIEW data acquisition system (with voltage amplifier) was used to drive the LC cells. The data recorded by the CCD camera was analyzed by a computer. Figure 3 shows the focusing properties of configurations A and B, as recorded by the CCD camera. Figures 3(a) and 3(b) show the images for configuration B at $V = 0$ and 180 V_{rms}, respectively. The measured focal length is 5 cm. The experimental results imply that configuration B has a better overall performance than A due to its larger number of fringe patterns (results not shown) and tighter focus, but its operating voltage is higher. To reduce voltage while maintaining a large aperture size, we could reduce the

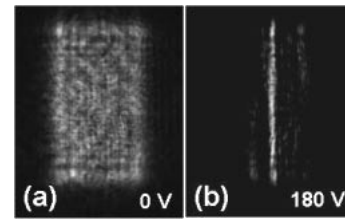


Fig. 3. Focusing properties of LC cylindrical lens recorded by CCD camera at different operating voltages for configuration B at 5 cm. (a) $V = 0$, and (b) $V = 180$ V_{rms}. $\lambda = 633$ nm.

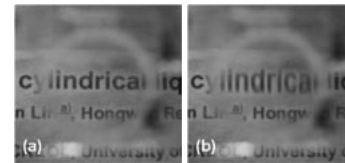


Fig. 4. White light imaging properties of cylindrical LC lenses of configuration B. (a) $V = 0$ V_{rms}, and (b) $V = 180$ V_{rms}. Slit width $a = 2$ mm.

glass substrate thickness or use a liquid crystal with a higher birefringence and a larger dielectric anisotropy.¹¹⁾

The cylindrical LC lens of the configuration B has a shorter focal length than that of configuration A because double-slit electrodes generate a steeper electric field gradient. Figure 4 shows the imaging properties of the lens using configuration B. In this experiment, the cylindrical lens was used to image the word "cylindrical" through a linear polarizer whose polarization axis is parallel to the slit direction of the LC lens. Without voltage, the word "cylindrical" is not magnified, as shown in Fig. 4(a). At $V = 180$ V_{rms}, the image is magnified only in the vertical dimension, as demonstrated in Fig. 4(b).

In conclusion, we have studied the light-focusing properties of cylindrical LC lenses of four different electrode configurations. The simulation results agree reasonably well with experimental results. The results suggest that a LC lens with a small focal length can be obtained by putting the electrodes on the outer surfaces of both substrates. The tradeoff is a higher operating voltage. Configuration B has the best overall performance.

This work is supported by the DARPA BOSS program under Contract No. W911NF04C0048.

- 1) S. T. Kowel, D. S. Cleverly and P. G. Kornreich: *Appl. Opt.* **23** (1984) 278.
- 2) N. A. Riza and M. C. DeJule: *Opt. Lett.* **19** (1994) 1013.
- 3) W. W. Chan and S. T. Kowel: *Appl. Opt.* **36** (1997) 8958.
- 4) O. A. Zayzkin, M. Y. Loktev, G. D. Love and A. F. Naumov: *Proc. SPIE* **3983** (1999) 112.
- 5) Z. He, T. Nose and S. Sato: *Jpn. J. Appl. Phys.* **33** (1994) 1091.
- 6) Z. He, T. Nose and S. Sato: *Jpn. J. Appl. Phys.* **34** (1995) 2392.
- 7) T. Nose, Y. Yamada and S. Sato: *Jpn. J. Appl. Phys.* **39** (2000) 6383.
- 8) H. Ren, Y. H. Fan, S. Gauza and S. T. Wu: *Jpn. J. Appl. Phys.* **43** (2004) 652.
- 9) S. Gauza, H. Wang, C. H. Wen, S. T. Wu, A. J. Seed and R. Dabrowski: *Jpn. J. Appl. Phys.* **42** (2003) 3463.
- 10) O. A. Zayzkin, M. Y. Loktev, G. D. Love and A. F. Naumov: *Proc. SPIE* **3983** (1999) 112.
- 11) S. T. Wu and D. K. Yang: *Reflective Liquid Crystal Displays* (Wiley, New York, 2001).